

# ИССЛЕДОВАНИЕ КОРРЕКЦИИ ХРОМАТИЧЕСКИХ АБЕРРАЦИЙ ДЛЯ ЦИФРОВЫХ ИЗОБРАЖЕНИЙ ГЛАЗНОГО ДНА

**В. Якстыс<sup>1</sup>, В. Марцинкевичюс<sup>1</sup>, П. Трейгис<sup>2</sup>**

---

<sup>1</sup>*Вильнюсский университет, Институт математики и информатики  
Вильнюс, Литва*

<sup>2</sup>*Вильнюсский университет, Институт математики и информатики  
Вильнюсский технический университет имени Гедиминаса  
Вильнюс, Литва*

*e-mail: [vytautas.jakstys@mii.vu.lt](mailto:vytautas.jakstys@mii.vu.lt), [virginijus.marcinkevicius@mii.vu.lt](mailto:virginijus.marcinkevicius@mii.vu.lt),  
[povilas.treigys@mii.vu.lt](mailto:povilas.treigys@mii.vu.lt)*

В данной работе основное внимание уделяется боковой коррекции хроматических aberrаций на снимках, сделанных камерой Optomed SmartScope M5. Эта портативная камера не имеет хроматических объективов. Когда в фотокамере нет хроматических объективов, необходимо использовать алгоритмы обработки изображений для боковой коррекции хроматических aberrаций. Эти алгоритмы пытаются масштабировать бахромчатые цветовые каналы таким образом, чтобы в конечном изображении все каналы пространственно перекрывали друг друга правильно.

Мы стремимся перестроить различные цветовые каналы. Это достигается за счет нахождения фокусного центра с помощью квазиньютоновского метода с использованием фильтра Gaussian Blur для разделения каналов и с использованием модели коррекции с минимизацией Левенберга – Марквардта. Были протестированы три различных модели коррекции для устранения хроматических aberrаций: простые (сдвига и масштаба), аффинные и проективные.

*Ключевые слова:* хроматические aberrации; изображения глазного дна; калибровка; повышение качества изображения; цифровые изображения.

## THE INVESTIGATION OF CHROMATIC ABERRATION CORRECTION FOR DIGITAL EYE FUNDUS IMAGES

**V. Jakštys<sup>1</sup>, V. Marcinkevičius<sup>1</sup>, P. Treigys<sup>2</sup>**

---

<sup>1</sup>*Vilnius University, Institute of Mathematics and Informatics  
Akademijos st. 4, LT-08663 Vilnius, Lithuania*

<sup>2</sup>*Vilnius University, Institute of Mathematics and Informatics  
Vilnius Gediminas Technical University  
Akademijos st. 4, LT-08663 Vilnius, Lithuania*

This paper focuses on the lateral chromatic aberration correction in images captured with Optomed SmartScope M5 camera. This portable non-mydratic eye fundus orbital camera does not have chromatic lenses. When photo camera system is designed

without chromatic lenses, it is necessary to apply image processing algorithms for lateral chromatic aberration effect correction. These algorithms try to scale the fringed colour channels so that all channels spatially overlap each other correctly in the final image.

We seek to realign different colour channels. This is achieved by: finding a focus centre using Quasi Newton method with Gaussian Blur filter to separate channels and using correction model with Levenberg – Marquardt minimization. Three different correction models were tested to eliminate the chromatic aberrations: simple (shift and scale), affine and projective.

*Keywords:* chromatic aberration; eye fundus images; calibration; image enhancement; digital images.

## INTRODUCTION

Chromatic aberration or focal distortion happens when different wavelength do not line up across the entire image. The result of this effect is an image with poor contrast and coloured fringes at edges. In general, it is not possible to create an optical system where there are no aberrations. Every lens tends to have various amounts of chromatic distortion. Nowadays the camera is used in many fields and is very important to make the device as small as possible. For this reason, it is very difficult to mechanically eliminate chromatic aberrations, so it is important to develop algorithms to eliminate chromatic aberrations. There are two types of chromatic aberration: Longitudinal and Lateral. Longitudinal chromatic effect becomes evident when colours have foci in different focal planes and colours will have different degrees of sharpness. Lateral chromatic aberration is observed when different wavelengths are focused on same focal plane but placed adjacent one to another. In the absence of axial foci, all colours are in focus, however, the more magnification is, the more blurred image is seen and lateral chromatic aberration never shows up in the centre. Lens might or do have both of these effects.

Mechanically this effect can be eliminated by adding extra lenses [1, 2]. According to the Abbe number, lenses can be situated in a manner that red and blue colour focal planes would match each other while wavelength of other colours refraction coincidence as good as possible. But to add extra lenses can be quite expensive and not always effective for the zones farther from the optical centre. Active lens method [3] is based on a modification in the camera settings: like zoom, focus for each colour channel. But this method is not practical because it needs to capture three photos of each channel with different camera settings. Simple (shifts and a scale) model can be successful applied to eliminate lateral chromatic aberration from fisheye lenses [4]. Other approaches [5–8] eliminate only the lateral chromatic aberration problem. These algorithms try to scale the fringed colour channels so that all channels spatially overlap each other correctly on the final image.

This study deals with images obtained with a portable Optomed SmartScope M5 non-mydiatic eye fundus orbital camera. This camera does not have chromatic lens installed and that results in: blurred vasculature; indefinite boundary of optic nerve disc; artificial colour appearance. As this camera does not have chromatic lenses, it should be eliminated by applying image processing algorithm for chromatic aberration effect correction.

Next section presents chromatic aberration type detection, the third – chromatic aberration correction method, the forth – evaluation of the correction models and the last – conclusions.

## CHROMATIC ABERRATION TYPE DETECTION

A calibration pattern must be chosen in order to detect chromatic aberration type. Chessboard and circles patterns with two different square sizes of  $8 \times 8$  pixels and  $4 \times 4$  pixels (e. g. fig. 1 left side) were used in our calibration experiments.

These calibration images were photographed with SmartScope M5 Optomed portable eye fundus camera at 8 cm distance from the camera objective. Size of obtained images is  $1920 \times 1440$  pixels. Resolution of the calibration pattern is 20,34 pixels per square centimetre. The calibration images (fig. 1, right side) shows that the camera has lateral chromatic aberration.

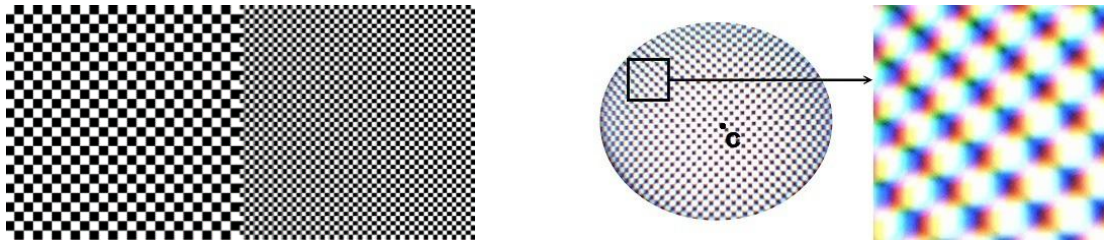


Fig. 1. Calibration patterns. From left to right: original calibration patterns, the patterns captured with SmartScope M5 camera

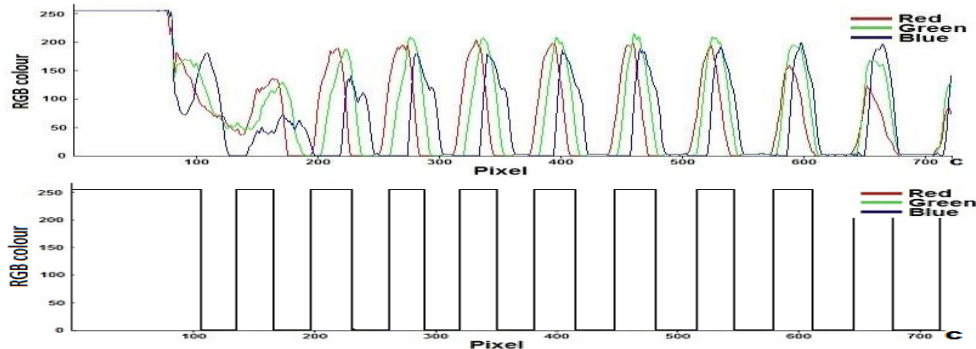


Fig. 2. Colours overlapping. From top to bottom: RGB colours intensities along horizontal line from border to a centre of the image, RGB colours intensities in ideal model

In fig. 2, upper graph illustrates RGB colours intensities along horizontal section of the captured pattern that section starts from border to a centre (C). It can be observed that magnitude of misalignment between channels increases when moving farther from the centre. If green channel is taken as reference, then it can be observed that red channel is shifted to the left and blue channel is shifted to the right. This means that red channel should be compressed and blue channel should be expanded. Lower graph of fig. 2 illustrates how channel positions should look like – all colours overlap each other without any mismatches.

## LATERAL CHROMATIC ABERRATION CORRECTION METHOD

Lateral chromatic aberration correction method for the camera is proposed in this paper. The method uses calibration images of chessboard or circles patterns that are taken by the camera and applies different technics to minimize lateral chromatic aberration effect. The method steps are as follows:

**Step 1.** Assume green channel is aberration free one. In order to see chromatic aberration intensities of green channel are subtracted from red and blue channels. The result is intensity images: G–R (green-red) (fig. 3, a) and G–B (green-blue). Two aberration

centres can be located by using these images. Similar technique using subtraction was first used by Luhmann [9].

- Step 2.** A picture received from the camera has ellipse within. This ellipse is always lying in the same position and axes of the ellipse are parallel to borders of the picture. Horizontal and vertical scans were performed to find the ellipse axis ends and calculate the centre of the ellipse.
- Step 3.** Square  $l \times l$  is inscribed at the centre of the intensity image (fig. 3, b). Length of the square border is  $l = \sqrt{2} \cdot a$ , where  $a$  – minor semiaxis of the ellipse.
- Step 4.** Gaussian blur with standard deviation of 64 was applied to form uneven surface of image intensities  $I(x, y)$  (fig. 3, c).
- Step 5.** Objective function (1) is used to locate aberration centre  $(x_c, y_c)$ . This function was minimized with Quasi Newton method [10]. fig. 3, c) and 3, d) show an example of starting position (white square centre) and located aberration centre (dashed square centre).

$$F(x_c, y_c) = \sum_{x=-\frac{l}{8}}^{\frac{l}{8}} \sum_{y=-\frac{l}{8}}^{\frac{l}{8}} I(x + x_c, y + y_c), \quad (1)$$

where  $l$  is image border size,  $I(x, y)$  – intensity value at point  $(x, y)$ .

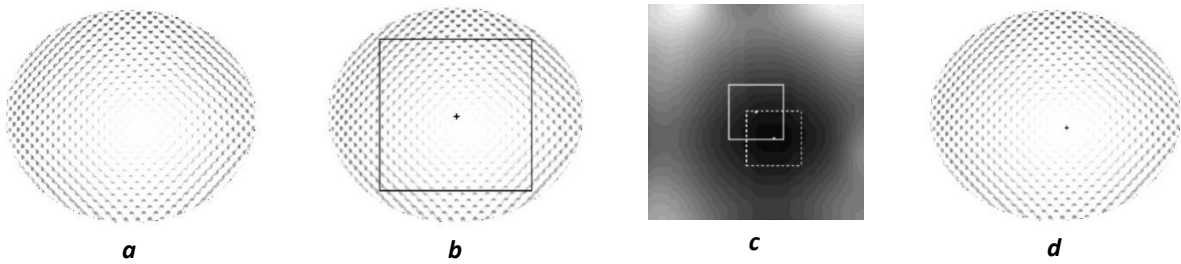


Fig. 3. Finding of aberration centre in G-R image: a – G-R image; b – inscribed square; c – the image after Gaussian blur filter; d – located aberration centre

- Step 6.** Calculation of chromatic aberration correction models. These models are calculated for red and blue colour channels by minimising objective function (2) with Levenberg – Marquardt algorithm (LMA) [11]:

$$E_{abr}(G, R) = \sum_{x=0}^{l_x} \sum_{y=0}^{l_y} (I_G(x, y) - I_R(x, y))^2, \quad (2)$$

where  $l_x$  is width and  $l_y$  is high of the image;  $I_G(x, y)$  is intensity of green colour channel;  $I_R(x, y)$  is intensity of red colour channel. Same formula is applied for blue colour channel.

- Step 7.** Correction models are applied on the image.

Three different chromatic aberration correction models were evaluated in this paper:

- Simple model included shifts ( $a_1$  and  $a_2$ ) and a scale ( $a_0$ ):
$$x_{corr} = a_0(x - x_c) + a_1; y_{corr} = a_0(y - y_c) + a_2. \quad (3)$$
- The affine model consisted of six parameters:
$$x_{corr} = a_0(x - x_c) + a_1(y - y_c) + a_2; y_{corr} = a_3(x - x_c) + a_4(y - y_c) + a_5. \quad (4)$$
- The projective model with 8 parameters:
$$x_{corr} = \frac{a_0(x - x_c) + a_1(y - y_c) + a_2}{a_6(x - x_c) + a_7(y - y_c) + 1}; \quad y_{corr} = \frac{a_3(x - x_c) + a_4(y - y_c) + a_5}{a_6(x - x_c) + a_7(y - y_c) + 1}; \quad (5)$$

where  $a_0, \dots, a_7$  – are coefficients,  $x, y$  – coordinates of some image point;  $x_c, y_c$  – coordinates of aberration centre.

## EVALUATION OF THE CORRECTION MODELS

Chessboards and circles patterns (fig. 1, left side) were used for evaluation of three models (simple, affine and projective) of the method. Results show (table) that affine and simple models give the best results. Although the projective model has more parameters, but correction ration compare to an image without correction ( $E_{abr\_wc}$ ) is small.

Correction models results

| Patterns                          | Model              | $E_{abr}(G, R)$  | $E_{abr}(G, B)$  | $E_{abr}(G, R) / E_{abr\_wc}(G, R)$ | $E_{abr}(G, B) / E_{abr\_wc}(G, B)$ |
|-----------------------------------|--------------------|------------------|------------------|-------------------------------------|-------------------------------------|
| Circle sizes of $8 \times 8$      | Without correction | 3007038390       | 3141114954       | 1                                   | 1                                   |
|                                   | Simple model       | 636243312        | 481400880        | 4,726240                            | 6,524946                            |
|                                   | Affine model       | <b>635779099</b> | <b>481547804</b> | <b>4,729691</b>                     | <b>6,522956</b>                     |
|                                   | Projective model   | 2048576366       | 2302893345       | 1,467867                            | 1,363986                            |
| Circle sizes of $4 \times 4$      | Without correction | 1553610155       | 1865208813       | 1                                   | 1                                   |
|                                   | Simple model       | 303646913        | 411273669        | 5,116502                            | 4,535201                            |
|                                   | Affine model       | <b>300054877</b> | <b>410935497</b> | <b>5,177753</b>                     | <b>4,538933</b>                     |
|                                   | Projective model   | 997318646        | 1520371014       | 1,557787                            | 1,226812                            |
| Chessboards sizes of $8 \times 8$ | Without correction | 4897794724       | 3699356794       | 1                                   | 1                                   |
|                                   | Simple model       | 848014213        | 653165015        | 5,775605                            | 5,66374                             |
|                                   | Affine model       | <b>847407887</b> | <b>644379388</b> | <b>5,779737</b>                     | <b>5,740961</b>                     |
|                                   | Projective model   | 3579515617       | 2987642401       | 1,368284                            | 1,238219                            |
| Chessboards sizes of $4 \times 4$ | Without correction | 2681361084       | 1936706713       | 1                                   | 1                                   |
|                                   | Simple model       | 621410209        | 332189605        | 4,314961                            | 5,830124                            |
|                                   | Affine model       | <b>615706115</b> | <b>329837539</b> | <b>4,354937</b>                     | <b>5,871699</b>                     |
|                                   | Projective model   | 1777871897       | 1483023471       | 1,508186                            | 1,305918                            |

Calibration image after applied achromatic aberration correction method with the affine model can be seen in fig. 4.

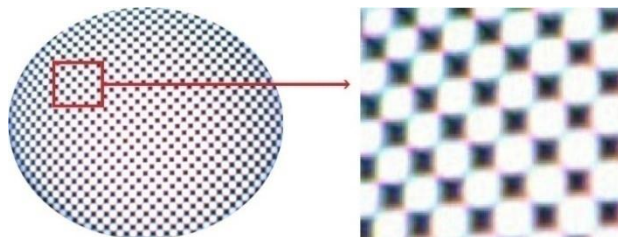


Fig. 4. Calibration image corrected with the affine calibration model

## CONCLUSIONS

The investigation of chessboard and circles pattern images has shown that Optomed SmartScope M5 camera lens produce significant lateral chromatic aberration effect. In this

paper, evaluation of the lateral chromatic aberration correction method with different chromatic aberration correction models (simple, affine, projective) was performed and the following conclusions were achieved:

- The method with affine model gives the best result. Objective function  $E_{abr}$  value is 4,35 – 6,52 times better than without correction.
- The Affine model is only slightly better (0,07 – 1,2 %) than the simple model. Nevertheless, the simple model is sufficient enough when calculation speed is required.
- The projective model has most parameters, so optimisation of these parameters is very difficult. Gradient descend method simply have been falling in to a local minimum, because that surfaces of optimisation functions  $E_{abr}$  are very sharp.

## LITERATURE

1. Kidger J. The Importance of Aberration Theory in Understanding Lens Design // Proceedings of the SPIE, 1997. P. 26–33.
2. Aberration Theory and Correction of Optical Systems / H. Gross [et al.] // Herbert Gross. Handbook of Optical Systems. 2007.
3. Willson G., Shafer Steven A. Proc. Active Lens Control for High Precision Computer Imaging // IEEE International Conference on Robotics and Automation (ICRA '91) / 1991. P. 2063–2070.
4. Pöntinen P. Study on Chromatic Aberration of two Fisheye Lenses // International Society for Photogrammetry and Remote Sensing. 2012. Vol. 37. P. 1682–1750.
5. Rudakova V., Monasse P. Precise Correction of Lateral Chromatic Aberration in Images // Image and Video Technology. 2013. Vol. 8333. P. 12–22.
6. Chung S-W., Kim B-K., Song W-J. Removing Chromatic Aberration by Digital Image Processing // Optical Engineering. 2010. Vol. 49.
7. Cecchetto B. Correction of Chromatic Aberration from a Single Image Using Keypoints // Computer Science 525, 2014.
8. Kang S. Automatic Removal of Chromatic Aberration from a Single Image // IEEE Conference on Computer Vision and Pattern Recognition, 2007. P. 1–8.
9. Luhmann T., Hastedt H. Modelling of Chromatic Aberration for High Precision Photogrammetry. Tecklenburg, Werner // International Society for Photogrammetry and Remote Sensing, 2006. Vol. 36.
10. Schoenberg R. Optimization with the Quasi-Newton Method // Schoenberg, Ronald, 2001.
11. More J. The Levenberg-Marquardt Algorithm: Implementation and Theory // Numerical Analysis. 1977. P. 105–116.